

# Orbital Orders and non-Fermi Liquid in Moiré systems

Yichen Xu,<sup>1</sup> Xiao-Chuan Wu,<sup>1</sup> Chao-Ming Jian,<sup>2</sup> and Cenke Xu<sup>1</sup>

<sup>1</sup>*Department of Physics, University of California, Santa Barbara, CA 93106, USA*

<sup>2</sup>*Station Q, Microsoft, Santa Barbara, California 93106-6105, USA*

Motivated by recent experiments, we study three different orbital orders that potentially can happen in the Moiré systems: (1) the nematic order; (2) the valley polarization; and (3) the “compass order”. Each order parameter spontaneously breaks part of the spatial symmetries of the system. We analyze the quantum fluctuation close to the order-disorder transition of these order parameters. Especially, we recognize that the symmetry of the Moiré systems leads to crucial difference of the effective theory describing the nematic order from the standard Hertz-Millis theory of other systems. We also demonstrate that this key difference may be responsible for the recently observed non-Fermi liquid behavior at commensurate fractional fillings in the twisted bilayer graphene. We identify the competing order of the superconductor observed in the Moiré system as either the valley polarization or the compass order.

PACS numbers:

Systems with Moiré superlattice have surprised the condensed matter community with a plethora of physics phenomena, supposedly due to the narrowness of the minibands in the Moiré mini Brillouin zone [1–7]. Correlated insulator at fractional fillings [8, 9], high temperature superconductor (compared with the miniband width) [1–3, 10–15], quantum anomalous Hall effect [16–19], strange metal (non-Fermi liquid) [20, 21], competing orders [22], spin-triplet pairing [1–3, 23] have all been reported in recent experiments on Moiré systems. Many of these phenomena may have to do with order parameters with nontrivial transformations under spatial symmetries, *i.e.* orbital orders. For example, the quantum anomalous Hall effect definitely requires valley polarization because the Chern numbers of two degenerate minibands from two different valleys cancel each other due to symmetry [16–19]. Also, strong signature of nematic anisotropy was found in recent experiments on twisted bilayer graphene [22]. Mean field studies of orbital orders in models related to Moiré systems have also been pursued [24]. In this work we will discuss three different kinds of orbital orders, *i.e.* (1) the nematic order, (2) valley polarization, and (3) “compass order”, which break different spatial symmetries. We will focus on the order-disorder quantum phase transition of these order parameters, and especially how the quantum fluctuations of these order parameters affect the electrons. We demonstrate that the nematic order fluctuation may be responsible for the observed non-Fermi liquid behavior, while the valley polarization and compass order will likely strongly compete with the superconductor.

## THREE ORBITAL ORDERS

In all the Moiré systems discovered so far, the most general microscopic symmetry is  $C_3 \times \mathcal{T}$ , where  $\mathcal{T}$  is an effective time-reversal symmetry which is a product

between the ordinary time-reversal and a spin-flipping, hence this effective time-reversal symmetry is preserved even when the system is in a background Zeeman field. Under this symmetry, the Fermi surface of the miniband from each valley only has a  $C_3$  symmetry, and  $\mathcal{T}$  interchanges the two valleys. The dispersion of the minibands from the two valleys satisfy  $\varepsilon_1(\vec{k}) = \varepsilon_2(-\vec{k})$ , where the subscript is the valley index. Different Moiré systems have different extra symmetries, for example the twisted bilayer graphene (TBG) without alignment with the BN has an inversion symmetry  $\mathcal{I}$ , while the trilayer graphene and h-BN heterostructure has a reflection symmetry  $\mathcal{P}$  [25]. Both  $\mathcal{I}$  and  $\mathcal{P}$  interchange the two valleys [25–27]. We will take the TBG as an example, and assume the symmetry of our system is  $C_3 \times \mathcal{T} \times \mathcal{I}$ . Under these spatial symmetries, the momenta and electron operators transform as

$$C_3 : (k_x + ik_y) \rightarrow e^{i2\pi/3}(k_x + ik_y);$$

$$\mathcal{T} : c_{a,\vec{k}} \rightarrow \tau_{ab}^1 c_{b,-\vec{k}}, \quad \mathcal{I} : c_{a,\vec{k}} \rightarrow \tau_{ab}^1 c_{b,-\vec{k}}. \quad (1)$$

In this work we will discuss three different orbital orders, each breaking different subgroups of the entire symmetry  $C_3 \times \mathcal{T} \times \mathcal{I}$ .

The first orbital order we will consider is the nematic order  $\phi$  which is a complex scalar order parameter. The microscopic operator of the nematic order parameter in a two dimensional ( $2d$ ) rotational invariant system can be written as [28]

$$\hat{\phi}(\vec{x}) \sim \psi^\dagger(\vec{x})(\partial_x^2 - \partial_y^2 + i2\partial_x\partial_y)\psi(\vec{x}) \quad (2)$$

where  $\psi(x)$  is the real space electron operator, it is an order parameter with zero or small momentum compared with the Fermi wave vector. In our case the zero momentum nematic order parameter can be represented as

$$\hat{\phi} \sim \sum_{\vec{k}} c_{1,\vec{k}}^\dagger (k_x^2 - k_y^2 + 2ik_x k_y + \alpha(k_x - ik_y)) c_{1,\vec{k}}$$

$$+ \sum_{\vec{k}} c_{2,\vec{k}}^\dagger (k_x^2 - k_y^2 + 2ik_x k_y - \alpha(k_x - ik_y)) c_{2,\vec{k}} \quad (3)$$

with real  $\alpha$ . Since the Fermi surface on each valley only has a  $C_3$  symmetry, the  $d_{x^2-y^2} + id_{xy}$  order parameter with angular momentum (+2) will mix with a  $p_x - ip_y$  order parameter with angular momentum (-1). The nematic order parameter  $\phi \sim \langle \hat{\phi} \rangle$  transforms under the symmetries as

$$C_3 : \phi \rightarrow e^{i2\pi/3} \phi; \quad \mathcal{T} : \phi \rightarrow \phi^*, \quad \mathcal{I} : \phi \rightarrow \phi. \quad (4)$$

A nonzero condensate of  $\phi$  will break the symmetries down to  $\mathcal{T}$  and  $\mathcal{I}$  only, and in this sense we can still refer to  $\phi$  as a nematic order parameter. Nematic order has been found in many condensed matter systems (for a review see Ref. 29), and strong signature of the existence of nematic order was recently reported in TBG [22].

The second orbital order we will discuss is the valley polarization  $\Phi$ , which corresponds to an operator

$$\hat{\Phi} \sim \sum_{\vec{k}} c_{1,\vec{k}}^\dagger c_{1,\vec{k}} - c_{2,\vec{k}}^\dagger c_{2,\vec{k}}. \quad (5)$$

A valley polarization  $\Phi \sim \langle \hat{\Phi} \rangle$  is an Ising like order parameter. A nonzero  $\Phi$  will cause imbalance of the electron density between the two valleys, and it may lead to the quantum anomalous Hall effect [16–19].  $\Phi$  preserves the  $C_3$  symmetry, but breaks both  $\mathcal{T}$  and  $\mathcal{I}$ .

The last order parameter is the ‘‘compass order’’ which is again a complex scalar order parameter. The compass order can be represented as

$$\begin{aligned} \hat{\varphi} \sim & \sum_{\vec{k}} c_{1,\vec{k}}^\dagger (k_x^2 - k_y^2 + 2ik_x k_y + \alpha(k_x - ik_y)) c_{1,\vec{k}} \\ & - \sum_{\vec{k}} c_{2,\vec{k}}^\dagger (k_x^2 - k_y^2 + 2ik_x k_y - \alpha(k_x - ik_y)) c_{2,\vec{k}} \end{aligned} \quad (6)$$

Under the symmetry actions, the compass order parameter  $\varphi \sim \langle \hat{\varphi} \rangle$  transforms as

$$C_3 : \varphi \rightarrow e^{i2\pi/3} \varphi; \quad \mathcal{T} : \varphi \rightarrow -\varphi^*, \quad \mathcal{I} : \varphi \rightarrow -\varphi. \quad (7)$$

The symmetry of  $\varphi$  implies that it can be viewed as  $\varphi \sim \phi\Phi$  in a Ginzburg-Landau type of analysis.

## NEMATIC ORDER

Normally when an order parameter with zero or small momentum couples to the Fermi surface, the dynamics of the order parameter is over-damped at low frequency according to the standard Hertz-Millis theory [30, 31]. The nematic order parameter is slightly more complicated, when coupled to a circular Fermi surface, the dynamics of the nematic order parameter is decomposed into

a transverse mode and longitudinal mode, and only the longitudinal mode is over-damped. The separation of the two modes was computed explicitly in Ref. 28, whose physical picture can be understood as following. Consider a general order parameter with small momentum  $\vec{q}$ , then the over-damping of this mode comes from its coupling with the patch of Fermi surface where the tangential direction is parallel with  $\vec{q}$ . For a circular Fermi surface, without loss of generality, let us assume  $\vec{q} = (q_x, 0)$ , then the Fermi patches that cause over-damping locate at  $\vec{k}_f \sim \pm \hat{y}$ . But  $\text{Im}[\phi]$  defined previously has nodes along the  $\pm \hat{y}$  direction (rotational invariance guarantees that the ‘‘tangential patch’’ of the Fermi surface coincides with the node of the transverse mode), hence  $\text{Im}[\phi]_{\vec{q}}$  with  $\vec{q} = (q_x, 0)$  is not over-damped.

But now the symmetry of the system, especially the fact that the  $d$ -wave order parameter mixes with the  $p$ -wave order parameter, no longer guarantees that for any small momentum  $\vec{q}$  the ‘‘tangential patch’’ of the Fermi surface coincides with the node of the order parameter, hence  $\phi$  is always over-damped, which can be shown with explicit calculations following Ref. 28. Thus we will start with the following Hertz-Millis type of action for the nematic order parameter  $\phi$ :

$$\begin{aligned} \mathcal{S}_b = & \sum_{\vec{q}, \omega} \phi_{\vec{q}, \omega}^* \left( \frac{|\omega|}{q} + q^2 + r \right) \phi_{\vec{q}, \omega} \\ & + \int d^2 x d\tau u (\phi^3 + \phi^{*3}) + g |\phi|^4. \end{aligned} \quad (8)$$

For convenience we have written the second line of the action in the Euclidean space-time while the first line in the momentum and Matsubara frequency space. Also, since the U(1) rotation of  $\phi$  is in fact a spatial rotation, there should be coupling between the direction of  $\vec{\phi} = (\text{Re}[\phi], \text{Im}[\phi])$  and direction of momentum, which we have ignored for simplicity. The action Eq. 8 is scaling invariant if we assign the following scaling dimensions to the parameters and field:

$$\begin{aligned} [\omega] = 3, \quad [q_x] = [q_y] = 1, \quad [r] = 2, \\ [\phi(\vec{x}, \tau)] = \frac{3}{2}, \quad [u] = \frac{1}{2}, \quad [g] = -1. \end{aligned} \quad (9)$$

At the level of the Hertz-Millis theory, normally the total space-time dimension is greater than the upper critical dimension and hence the theory will lead to a mean field transition (for a review see Ref. 32). While unlike the ordinary Hertz-Millis theory, in our current case there is a symmetry-allowed term  $u(\phi^3 + \phi^{*3})$  that is relevant even though the total space-time dimension is  $D = d + z = 5$ . Thus we need to perform analysis beyond the mean field theory.

The relevant  $u$  term breaks the U(1) symmetry of  $\phi$  down to a  $Z_3$  symmetry, which is the symmetry of a three-state clock model. Though a two dimensional

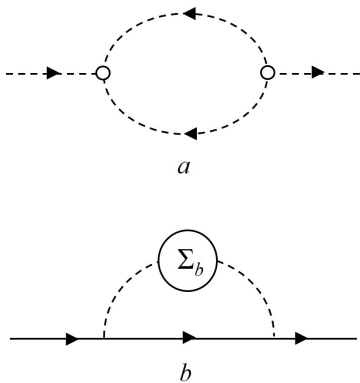


FIG. 1: *a*, the one-loop correction to the boson propagator from the  $u$  term in Eq. 8; *b*, the one-loop correction to the fermion propagator in Eq. 12.

three-state clock model (equivalent to a three-state Potts model) has a continuous transition and can be potentially described by the Ginzburg-Landau theory with a  $Z_3$  anisotropy on a U(1) order parameter [33], a mean field analysis of such Ginzburg-Landau theory would lead to a first order transition which occurs at  $r \sim u^2/g$ , hence the scaling analysis above can be applied when  $r$  is tuned close to the transition, and the energy scale  $\omega \gg (u^2/g)^{3/2}$ , *i.e.* when the order parameter can be viewed massless. We also need the energy scale to satisfy  $\omega < 1/g^3$  so the irrelevant coupling  $g$  is renormalized small enough. Hence as long as  $(u^2/g)^{3/2} \ll 1/g^3$ , there is a finite energy window where the analysis in this work applies.

Based on Eq. 8, if we take into account of the relevant perturbation  $u$ , in general the boson propagator reads

$$\begin{aligned} G_b(\omega, \vec{q}) &= \frac{1}{G_{b0}^{-1}(\omega, \vec{q}) + \Sigma_b(\omega, \vec{q})}, \\ G_{b0}^{-1}(\omega, \vec{q}) &= \frac{|\omega|}{q} + q^2. \end{aligned} \quad (10)$$

A full reliable analysis of Eq. 8 with the relevant perturbation  $u$  is difficult, we will first limit our study to the lowest nontrivial order of perturbation of  $u$ , later we will discuss other analysis. At the one-loop level (Fig. 3a), the boson self-energy  $\Sigma_b(\omega, \vec{p})$  reads

$$\begin{aligned} \Sigma_b &\sim u^2 \int d^2k d\nu G_{b0}(\nu, \vec{k}) G_{b0}(\omega + \nu, \vec{q} + \vec{k}), \\ &\sim \text{Const} + Au^2 \sqrt{|\omega|^{2/3} + cq^2} + \dots \end{aligned} \quad (11)$$

The behavior of the boson self-energy is consistent with power-counting of the loop integral. The cut-off dependent constant can be reabsorbed into  $r$ , and the ellipsis includes terms that are less dominant in the infrared.

Most importantly we need to analyze the effects of the boson-fermion coupling on the electrons. In the Hertz-Millis theory without the relevant  $u$  term in the boson

action, the one loop self-energy of the electron scales as  $\Sigma_f(\omega) \sim \text{sgn}[\omega]|\omega|^{2/3}$ . Following the standard practice, we expand the system at one patch of the Fermi surface. This one-patch theory breaks the  $C_3$  symmetry, hence the real and imaginary parts of  $\phi$  are no longer degenerate. Since we are most interested in the scaling behavior of the Fermion self-energy, we will consider a one component boson field with the dressed propagator and self-energy given by Eq. 11. The one-patch theory reads

$$\begin{aligned} \mathcal{S}_{bf} &= \sum_{\omega, \vec{k}} \psi_{\omega, \vec{k}}^\dagger (i\omega - v_f k_x - v k_y^2) \psi_{\omega, \vec{k}} \\ &+ \sum_{\omega, \vec{q}} u^2 \sqrt{|\omega|^{2/3} + cq^2} |\phi_{\omega, \vec{q}}|^2 \\ &+ \int d^2x d\tau g' \phi \psi^\dagger \psi. \end{aligned} \quad (12)$$

For this theory we need to use a different assignment of scaling dimensions [34, 35]:

$$\begin{aligned} [\omega] &= 3, \quad [k_x] = 2, \quad [k_y] = 1, \\ [\phi(\vec{x}, \tau)] &= \frac{5}{2}, \quad [\psi] = 2, \quad [g'] = -\frac{1}{2}. \end{aligned} \quad (13)$$

Also, suppose we include a  $\phi^3$  term in the Eq. 12, it would be irrelevant in this new convention of scaling.

The one-loop fermion self-energy (Fig. 3b) reads

$$\begin{aligned} \Sigma_f(\omega) &\sim \int d^2k d\nu G_{f0}(\nu, \vec{k}) G_b(\omega + \nu, \vec{k}) \\ &\sim \int d^2k d\nu \frac{1}{i\nu - v_f k_x - v k_y^2} \frac{1}{\sqrt{|\omega + \nu|^{2/3} + ck^2}} \\ &\sim i\omega \log\left(\frac{\Lambda}{|\omega|}\right), \end{aligned} \quad (14)$$

which is precisely the marginal fermi liquid behavior, and it is consistent with the simple power-counting of the loop integral. The marginal fermi liquid was proposed as a phenomenological theory for the strange metal phase (a non-Fermi liquid phase) of the cuprates high temperature superconductor [36]. After converting the Matsubara frequency to the real frequency, the imaginary part of the the fermion self-energy is proportional to  $|\omega|$ , which is consistent with the linear- $T$  scaling of the resistivity in the strange metal phase [36]. A similar strange metal behavior was observed in the TBG [20–22][50].

Because  $g'$  is an irrelevant perturbation in Eq. 12, higher order perturbation of  $g'$  in theory Eq. 12 is not expected to lead to more dominant correction to the fermion self-energy in the infrared, hence we no long need to worry about the infinite “planar diagram” problem in ordinary cases when an order parameter is coupled with a Fermi surface [35].

The results above are based on the one-loop result in the expansion of  $u$ . A full solution of the theory is expected to give us the following form of the full boson

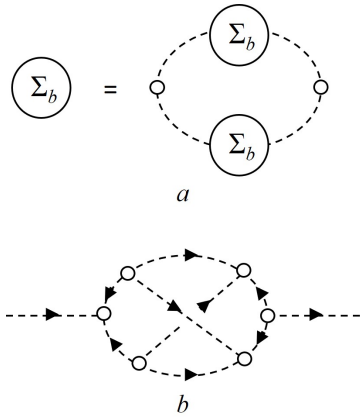


FIG. 2: *a*, the schematic representation of the Schwinger-Dyson equation; *b*, the example of vertex correction that is not summed in the Schwinger-Dyson equation.

self-energy

$$\Sigma_b(\omega, \vec{q}) \sim Q^{2-\eta} \quad (15)$$

with anomalous dimension  $\eta$ , where  $Q$  is the infrared cut-off that can be taken as  $\text{Max}[|\omega|^{1/3}, |\vec{q}|]$ . The one-loop result yields  $\eta = 1$ . Now the bosonic part of the boson-fermion coupling action Eq. 12 is replaced by

$$\mathcal{S}_b = \sum_{\omega, \vec{p}} \Sigma_b(\omega, \vec{q}) |\phi_{\omega, \vec{q}}|^2, \quad (16)$$

and the scaling of the boson-fermion coupling theory is modified as

$$[\omega] = 3, \quad [k_x] = 2, \quad [k_y] = 1, \\ [\phi(\vec{x}, \tau)] = \frac{4+\eta}{2}, \quad [\psi] = 2, \quad [g'] = -\frac{\eta}{2}. \quad (17)$$

Again the one-loop fermion self-energy should scale as

$$\Sigma_f(\omega) \sim i\omega |\omega|^{\frac{\eta-1}{3}}. \quad (18)$$

As long as  $\eta > 0$ , the boson-fermion coupling  $g'$  in Eq. 12 is still irrelevant, hence higher order fermion self-energy diagrams from the boson-fermion coupling theory are not expected to change Eq. 18 in the infrared.

Although we cannot solve the theory completely, one approximate way of evaluating the anomalous dimension  $\eta$  is through the Schwinger-Dyson (SD) equation, which sums a subset of the Feynman diagrams Fig. 2*a*:

$$\Sigma_b \sim u^2 \int d^2k d\nu G_b(\nu, \vec{k}) G_b(\omega + \nu, \vec{q} + \vec{k}), \\ G_b^{-1} = G_{b0}^{-1} + \Sigma_b. \quad (19)$$

Here we have ignored the vertex correction from the full SD equation (For example, vertex correction Fig. 2*b*). The solution of this equation would yield  $\eta = 1/3$ , which will lead to a non-fermi liquid behavior that is in-between the standard Hertz-Millis theory and also the marginal fermi liquid.

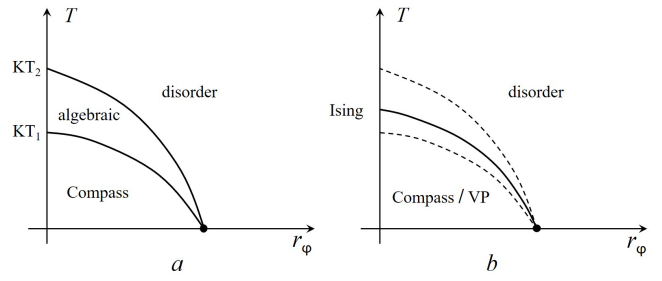


FIG. 3: *a*, the phase diagram when there is a compass order at zero temperature, there are two consecutive Kosterlitz-Thouless transitions at finite temperatures and an algebraic phase in between; *b*, once there is a background strain in the system, the compass order is identical to the valley polarization (VP) order, and hence there is only one Ising transition at finite temperature.

### VALLEY POLARIZATION AND COMPASS ORDER

The effective theory of the valley polarization order and compass order are more conventional Hertz-Millis theories whose analysis can be quoted from Ref. 32. The symmetry transformation of  $\varphi$  allows a term

$$u_6(\varphi^6 + \varphi^{*6}) \quad (20)$$

in the Ginzburg-Landau-Hertz-Millis theory, which is irrelevant in the infrared at the total space-time dimension  $D = 5$ . The three order parameters are coupled together in the effective theory, and the lowest order symmetry-allowed couplings are:

$$\mathcal{L}_{mix} = \dots + r_\phi |\phi|^2 + r_\varphi |\varphi|^2 + r_\Phi |\Phi|^2 \\ + v_1(\Phi\phi\varphi^* + h.c.) + v_2(\Phi\varphi^3 + h.c.) \\ + v_3\Phi^2|\phi|^2 + v_4\Phi^2|\varphi|^2. \quad (21)$$

A full exploration of the multi-dimensional parameter space will lead to a complex and rich phase diagram.

Recently evidence of strain that breaks the  $C_3$  rotation symmetry has been reported in Moiré systems [37], and the strain can potentially strongly affect the band structure [38]. With a background strain field, the nematic order parameter  $\phi$  acquires a nonzero expectation value, and hence  $\Phi$  and  $\varphi$  become the same order parameter through the coupling  $v_1$  in  $\mathcal{L}_{mix}$ .

At finite temperature, the nematic order and valley polarization will go through continuous transitions which correspond to the three-state potts and Ising conformal field theory with central charges  $4/5$  and  $1/2$  respectively. While if we start with a zero temperature compass order, the finite temperature physics can be mapped to a six-state clock model due to the  $u_6$  term mentioned previously in the Ginzburg-Landau theory of the compass

order. In this case while raising temperature the system will undergo two consecutive continuous Kosterlitz-Thouless transitions with an algebraic quasi-long range order in between. Within the algebraic phase, the scaling dimension of the compass order parameter  $[\varphi]$  is temperature dependent, and  $1/18 < [\varphi] < 1/8$ . The nematic order parameter  $\phi \sim \varphi^{*2}$  and valley polarization  $\Phi \sim \varphi^3 + \varphi^{*3}$  also have power-law correlation function in the algebraic phase, and their scaling dimensions are  $[\phi] = 4[\varphi]$ , and  $[\Phi] = 9[\varphi]$ . Hence a background strain which pins  $\phi$  is always a relevant perturbation in the algebraic phase, and will collapse the two Kosterlitz-Thouless transitions of  $\varphi$  into a single Ising transition of  $\Phi$ .

Signature of a hidden order which strongly competes with superconductor was observed experimentally [22]. Within the three orbital orders that we have discussed in this work, the valley polarization and compass order both obviously compete with the superconductor. The reason is that both these two order parameters break  $\mathcal{T}$  and  $\mathcal{I}$ , hence break the degeneracy between electrons at  $\vec{k}$  and  $-\vec{k}$  (the  $C_3$  symmetry alone does not protect this degeneracy), hence a nonzero  $\Phi$  or  $\varphi$  makes it difficult to form zero momentum Cooper pair. Of course, nonzero momentum pairing (pair density wave) is in principle possible, but unless there is compelling experimental evidence for this exotic pairing, we will assume that the superconductor in the Moiré system has zero momentum. Indeed, experiments so far show that superconductivity does not exist near the quantum anomalous Hall state observed in Moiré systems which at least requires either valley polarization or the compass order.

## FINAL REMARKS

In this work we studied three different orbital orders that may be responsible to some of the recently observed experimental phenomena in Moiré systems, such as the non-Fermi liquid and also competing order of the superconductor. Since the three different orbitals can interact with each other in the effective theory and lead to a complex and rich phase diagram, depending on the parameters different Moiré systems under different conditions may have different orbital orders. We demonstrate that the effective theory for the nematic order is beyond the standard Hertz-Millis theory. Numerical methods such as Ref. 39–41 are demanded to verify the results in the current work. We are also pursuing (in progress) a proper generalized renormalization group expansion such as Ref. 42–44, as well as analysis of the stability of nematic order transition against other orders such as superconductivity [45–48] in Moiré systems.

The authors thank Leon Balents, Steve Kivelson for helpful discussions. This work is supported by NSF Grant No. DMR-1920434, the David and Lucile Packard Foundation, and the Simons Foundation.

- 
- [1] C. Shen, N. Li, S. Wang, Y. Zhao, J. Tang, J. Liu, J. Tian, Y. Chu, K. Watanabe, T. Taniguchi, et al., arXiv:1903.06952 (2019).
  - [2] X. Liu, Z. Hao, E. Khalaf, J. Y. Lee, K. Watanabe, T. Taniguchi, A. Vishwanath, and P. Kim, arXiv:1903.08130 (2019).
  - [3] Y. Cao, D. Rodan-Legrain, O. Rubies-Bigorda, J. M. Park, K. Watanabe, T. Taniguchi, and P. Jarillo-Herrero, arXiv:1903.08596 (2019).
  - [4] R. Bistritzer and A. H. MacDonald, Proceedings of the National Academy of Sciences **108**, 12233 (2011), ISSN 0027-8424, <http://www.pnas.org/content/108/30/12233.full.pdf>, URL <http://www.pnas.org/content/108/30/12233>.
  - [5] E. Suárez Morell, J. D. Correa, P. Vargas, M. Pacheco, and Z. Barticevic, Phys. Rev. B **82**, 121407 (2010), URL <https://link.aps.org/doi/10.1103/PhysRevB.82.121407>.
  - [6] S. Fang and E. Kaxiras, Phys. Rev. B **93**, 235153 (2016), URL <https://link.aps.org/doi/10.1103/PhysRevB.93.235153>.
  - [7] G. Trambly de Laissardière, D. Mayou, and L. Magaud, Phys. Rev. B **86**, 125413 (2012), URL <https://link.aps.org/doi/10.1103/PhysRevB.86.125413>.
  - [8] G. Chen, L. Jiang, S. Wu, B. Lv, H. Li, K. Watanabe, T. Taniguchi, Z. Shi, Y. Zhang, and F. Wang, arXiv:1803.01985 (2018).
  - [9] Y. Cao, V. Fatemi, A. Demir, S. Fang, S. L. Tomarken, J. Y. Luo, J. D. Sanchez-Yamagishi, K. Watanabe, T. Taniguchi, E. Kaxiras, et al., Nature **556**, 80 (2018).
  - [10] Y. Cao, V. Fatemi, S. Fang, K. Watanabe, T. Taniguchi, E. Kaxiras, and P. Jarillo-Herrero, Nature **556**, 43 (2018).
  - [11] M. Yankowitz, S. Chen, H. Polshyn, Y. Zhang, K. Watanabe, T. Taniguchi, D. Graf, A. F. Young, and C. R. Dean, Science **363**, 1059 (2019), ISSN 0036-8075, <http://science.sciencemag.org/content/363/6431/1059.full.pdf>, URL <http://science.sciencemag.org/content/363/6431/1059>.
  - [12] G. Chen, A. L. Sharpe, P. Gallagher, I. T. Rosen, E. Fox, L. Jiang, B. Lyu, H. Li, K. Watanabe, T. Taniguchi, et al., arXiv:1901.04621 (2019).
  - [13] A. L. Sharpe, E. J. Fox, A. W. Barnard, J. Finney, K. Watanabe, T. Taniguchi, M. A. Kastner, and D. Goldhaber-Gordon, arXiv:1901.03520 (2019).
  - [14] P. Kim, *Ferromagnetic superconductivity in twisted double bilayer graphene*, [http://online.kitp.ucsb.edu/online/bands\\_m19/kim/](http://online.kitp.ucsb.edu/online/bands_m19/kim/) (2019), Talks at KITP, Jan 15, 2019.
  - [15] X. Lu, P. Stepanov, W. Yang, M. Xie, M. A. Aamir, I. Das, C. Urgell, K. Watanabe, T. Taniguchi, G. Zhang, et al., arXiv:1903.06513 (2019).
  - [16] N. Bultinck, S. Chatterjee, and M. P. Zaletel, arXiv:1901.08110 (2019).
  - [17] Y.-H. Zhang, D. Mao, and T. Senthil, arXiv:1901.08209 (2019).
  - [18] G. Chen, A. L. Sharpe, E. J. Fox, Y.-H. Zhang, S. Wang, L. Jiang, B. Lyu, H. Li, K. Watanabe, T. Taniguchi, et al., arXiv:1905.06535 (2019).
  - [19] M. Serlin, C. L. Tschirhart, H. Polshyn, Y. Zhang, J. Zhu, K. Watanabe, T. Taniguchi, and L. B. Abd A. F. Young,

- arXiv:1907.00261 (2019).
- [20] Y. Cao, D. Chowdhury, D. Rodan-Legrain, O. Rubies-Bigord, K. Watanabe, T. Taniguchi, T. Senthil, and P. Jarillo-Herrero, arXiv:1901.03710 (2019).
- [21] H. Polshyn, M. Yankowitz, S. Chen, Y. Zhang, K. Watanabe, T. Taniguchi, C. R. Dean, and A. F. Young, arXiv:1902.00763 (2019).
- [22] P. Jarillo-Herrero, *Magic Angle Graphene Transport Phenomenology*, [http://online.kitp.ucsb.edu/online/bands\\_m19/jarilloherrero/](http://online.kitp.ucsb.edu/online/bands_m19/jarilloherrero/) (2019).
- [23] J. Y. Lee, E. Khalaf, S. Liu, X. Liu, Z. Hao, P. Kim, and A. Vishwanath, arXiv:1903.08130 (2019).
- [24] J. F. Dodaro, S. A. Kivelson, Y. Schattner, X. Q. Sun, and C. Wang, Phys. Rev. B **98**, 075154 (2018), URL <https://link.aps.org/doi/10.1103/PhysRevB.98.075154>.
- [25] H. C. Po, L. Zou, A. Vishwanath, and T. Senthil, Phys. Rev. X **8**, 031089 (2018), URL <https://link.aps.org/doi/10.1103/PhysRevX.8.031089>.
- [26] L. Zou, H. C. Po, A. Vishwanath, and T. Senthil, Phys. Rev. B **98**, 085435 (2018), URL <https://link.aps.org/doi/10.1103/PhysRevB.98.085435>.
- [27] Y.-H. Zhang and T. Senthil, arXiv:1809.05110 (2018).
- [28] V. Oganesyan, S. A. Kivelson, and E. Fradkin, Phys. Rev. B **64**, 195109 (2001), URL <https://link.aps.org/doi/10.1103/PhysRevB.64.195109>.
- [29] E. Fradkin, S. A. Kivelson, M. J. Lawler, J. P. Eisenstein, and A. P. Mackenzie, Annual Review of Condensed Matter Physics **1**, 153 (2010), <https://doi.org/10.1146/annurev-conmatphys-070909-103925>, URL <https://doi.org/10.1146/annurev-conmatphys-070909-103925>.
- [30] J. A. Hertz, Phys. Rev. B **14**, 1165 (1976), URL <https://link.aps.org/doi/10.1103/PhysRevB.14.1165>.
- [31] A. J. Millis, Phys. Rev. B **48**, 7183 (1993), URL <https://link.aps.org/doi/10.1103/PhysRevB.48.7183>.
- [32] H. v. Löhneysen, A. Rosch, M. Vojta, and P. Wölfle, Rev. Mod. Phys. **79**, 1015 (2007), URL <https://link.aps.org/doi/10.1103/RevModPhys.79.1015>.
- [33] F. Fucito and G. Parisi, J. Phys. A: Math. Gen. **14**, L507 (1981).
- [34] M. A. Metlitski and S. Sachdev, Phys. Rev. B **82**, 075127 (2010), URL <https://link.aps.org/doi/10.1103/PhysRevB.82.075127>.
- [35] S.-S. Lee, Phys. Rev. B **80**, 165102 (2009), URL <https://link.aps.org/doi/10.1103/PhysRevB.80.165102>.
- [36] C. M. Varma, P. B. Littlewood, S. Schmitt-Rink, E. Abrahams, and A. E. Ruckenstein, Phys. Rev. Lett. **63**, 1996 (1989), URL <https://link.aps.org/doi/10.1103/PhysRevLett.63.1996>.
- [37] Y. Xie, B. Lian, B. Jäck, X. Liu, C.-L. Chiu, K. Watanabe, T. Taniguchi, B. A. Bernevig, and A. Yazdani, Nature **572**, 101 (2019).
- [38] Z. Bi, N. F. Q. Yuan, and L. Fu, Phys. Rev. B **100**, 035448 (2019), URL <https://link.aps.org/doi/10.1103/PhysRevB.100.035448>.
- [39] Y. Schattner, S. Lederer, S. A. Kivelson, and E. Berg, Phys. Rev. X **6**, 031028 (2016), URL <https://link.aps.org/doi/10.1103/PhysRevX.6.031028>.
- [40] S. Lederer, Y. Schattner, E. Berg, and S. A. Kivelson, Proceedings of the National Academy of Sciences **114**, 4905 (2017), ISSN 0027-8424, <https://www.pnas.org/content/114/19/4905.full.pdf>, URL <https://www.pnas.org/content/114/19/4905>.
- [41] X. Y. Xu, Z. H. Liu, G. Pan, Y. Qi, K. Sun, and Z. Y. Meng, arXiv:1904.07355 (2019).
- [42] C. Nayak and F. Wilczek, Nuclear Physics B **417**, 359 (1994), ISSN 0550-3213, URL <http://www.sciencedirect.com/science/article/pii/0550321394904774>.
- [43] C. Nayak and F. Wilczek, Nuclear Physics B **430**, 534 (1994), ISSN 0550-3213, URL <http://www.sciencedirect.com/science/article/pii/0550321394901589>.
- [44] D. F. Mross, J. McGreevy, H. Liu, and T. Senthil, Phys. Rev. B **82**, 045121 (2010), URL <https://link.aps.org/doi/10.1103/PhysRevB.82.045121>.
- [45] M. A. Metlitski, D. F. Mross, S. Sachdev, and T. Senthil, Phys. Rev. B **91**, 115111 (2015), URL <https://link.aps.org/doi/10.1103/PhysRevB.91.115111>.
- [46] S. Lederer, Y. Schattner, E. Berg, and S. A. Kivelson, Phys. Rev. Lett. **114**, 097001 (2015), URL <https://link.aps.org/doi/10.1103/PhysRevLett.114.097001>.
- [47] J. Rech, C. Pépin, and A. V. Chubukov, Phys. Rev. B **74**, 195126 (2006), URL <https://link.aps.org/doi/10.1103/PhysRevB.74.195126>.
- [48] A. V. Chubukov, C. Pépin, and J. Rech, Phys. Rev. Lett. **92**, 147003 (2004), URL <https://link.aps.org/doi/10.1103/PhysRevLett.92.147003>.
- [49] F. Wu, E. Hwang, and S. Das Sarma, Phys. Rev. B **99**, 165112 (2019), URL <https://link.aps.org/doi/10.1103/PhysRevB.99.165112>.
- [50] It was suggested that a pure phonon-electron coupling can lead to a linear- $T$  resistivity in Moiré systems [21, 49], but it was argued in Ref. 20 that other mechanisms may be demanded to explain the observed data.